Theoretical Analysis of the Energy Gap Dependence of the Reconstituted B800 → B850 Excitation Energy Transfer Rate in Bacterial LH2 Complexes

A. Kimura and T. Kakitani*

Department of Physics, Graduate School of Science, Nagoya University, Furo-cho, Chikusa-ku, Nagoya 464-8602, Japan

Received: February 8, 2003; In Final Form: April 24, 2003

Theoretical analysis was carried out for a remarkable energy gap dependence of the rate of excitation energy transfer (EET) from reconstituted B800 to B850 in LH2 whose experimental data were published recently (Herek, J. L.; Fraser, N. J.; Pullerits, T.; Martinsson, P.; Polivka, T.; Scheer, H.; Cogdell, R. J.; Sundstrom, V. *Biophys. J.* **2000**, *78*, 2590). This energy gap dependence could not be explained by calculations using the generalized Förster theory. As an alternative method, we solved the generalized master equation for the population of the excited BChla molecules that are coupled inside the B850 ring and between B850 and B800 by adopting second-order perturbation theory for the memory function. Making use of the experimental data of optical absorption and fluorescence spectra of monomers and proper site energies in LH2, we could theoretically reproduce the above experimentally observed energy gap dependence of the EET rate very well. The result of the present analysis indicates that the rate-limiting step for the EET of B800 → B850 is the EET from the localized state of B800 mostly to the nearby BChla molecules with a site energy of about 810 nm in the B850 ring. A physical explanation of this result is discussed.

1. Introduction

Excitation energy transfer (EET) is a significant process in physics, chemistry, and biology. The EET in the antenna complex of a photosynthetic system plays a central role in collecting photoenergy.[1,2] The light-harvesting antenna system 2 (LH2) in photosynthetic purple bacteria *Rhodopseudomonas (Rps.) acidophila* is a nonameric circular aggregate of α,β-heterodimers, with each subunit noncovalently binding three bacteriochlorophylls. Namely, 18 and 9 bacteriochlorophyll a (BChla) molecules are respectively arranged in rings that absorb light of 850 or 800 nm and hence are called B850 and B800.[3] Light energy is absorbed by either B800 or B850. The light energy absorbed by B800 is transferred to B850 in 0.9 ps at room temperature. The excitation energy collected by B850 is transferred to the other LH2 or to the other kind of light-harvesting antenna system 1, LH1, and finally transferred to the special pair of the reaction center.[4] It is now well known that the largely red-shifted absorption band of B850 is due to exciton formation that extends over almost the whole ring.[5−11] The B800 absorption is a little red-shifted from that of Q_y band of the BChla monomer, ca. 770 nm. This small red shift is due to the interaction of BChla with the protein environment. The excited state of B800 was considered to be localized at a monomer.[6]

The mechanism of EET from B800 to B850 has been of great debate. Because the peak of the absorption band of B850 is largely separated from that of the emission band of B800, the overlap of the two spectra was once thought to be too small to explain the fast EET rate by Förster theory.[12] Instead, it was proposed that the optically forbidden exciton bands at higher energy levels of B850 would play a significant role in the EET.[13,14] The reason is that the interaction between the higher optically forbidden levels of B850 and the excited state of B800 does not necessarily become zero because of the large size of the donor and acceptor molecules. When the size of the donor and acceptor is comparable with the donor−acceptor distance, higher-order multipole−multipole interaction can be effective.[15] It was shown that this mechanism is effective in EET from the forbidden excited state of a carotenoid to bacteriochlorophyll.[16] The EET rate was calculated by summing the EET through many channels with the final states of both optically allowed and forbidden exciton states of B850.[13,14] The EET rate for each channel was calculated by the Förster mechanism based on Fermi's golden rule. This theory was called the generalized Förster theory.[14] Then, they theoretically obtained the EET rate,[14] which is comparable to the experimental value 0.7 ps for *Rb. sphaeroides* at room temperature.[17] Although this is one of many possible ways of explaining the experimental EET rate, it will not be conclusive because an excess number of parameters are involved in the calculation. So, we propose to check its mechanism further by making use of the systematic experimental data.

Under such a situation, a large volume of experimental data has been published recently.[18] The data are the energy gap dependence of the EET rate using the reconstituted B800−B850 system.[18] Namely, the B800 pigments in LH2 of *Rps. acidophila* were first depleted by incubating an LH2 sample in buffer containing triton TBG10. The obtained B850-only sample had an optical absorption peak at 850 nm but had no peak around 800 nm.[18,19] It was also confirmed that the B850 band has a long tail of considerable intensity on the shorter-wavelength side. Then, the B850-only sample was incubated with BChla, the BChla analogue, and chlorophyll a (Chla) or the Chla analogue (which are called tetraphyrrole pigments as a whole), producing the reconstituted B800−B850 complex. The reconstituted sample with BChla had a peak at 800 nm, similar to the native one, confirming that the reconstitution is correct. The reconstituted samples with tetrapyrrole pigments with shorter-wavelength absorption absorbed at wavelengths shorter than 800

* Corresponding author. E-mail: kakitani@allegro.phys.nagoya-u.ac.jp. Tel and Fax: +81-52-789-3528.

10.1021/jp034329t CCC: $25.00
Published on Web 07/09/2003

TABLE 1: Summary of the Experimental Data of the Q_y Absorption and Fluorescence Maximal Wavelengths and EET Time in Reconstituted LH2 of *Rps. Acidophilla*[18] [a]

B800 Site (Donor Site)

symbol	pigment	λ_{max}^{abs} (nm)	λ_{max}^{fl} (nm)	apparent energy gap $-\Delta G^a$ (cm^{-1})	site energy gap $-\Delta G^s$ (cm^{-1})	τ^{ex} (ps)	τ^{GM} (ps)	τ^{PM} (ps)
a	BChla	800	805	657	76	0.9 ± 0.1	0.83	0.84
b	Z_n-Bphea	794	799	750	169	0.8 ± 0.1	0.85	0.85
c	3-vinyl-BChla	765	770	1220	639	1.4 ± 0.2	1.56	1.58
d	3′-OH−BChla	753	758	1430	849	1.8 ± 0.2	1.66	1.67
e	3-acetyl-Chla	694	698	2560	1980	4.4 ± 0.5	3.49	3.55
f	Chla	670	674	3070	2490	8.3 ± 0.5	9.84	10.21

B850 Site (Acceptor Site)

λ_{max}^{abs} (nm)	
exciton state	monomer state
850	810

[a] The apparent energy gap $-\Delta G^a$ was calculated from the difference between the fluoresence energy at the B800 site and the absorption energy of the exciton state of the B850 site. The site energy gap was calculated from the difference between the fluorescence energy at the B850 site and the absorption energy of the monomer state at the B850 site. The monomer state energy of the B850 site was calculated so that the 850-nm allowed exciton band is reproduced when the intermolecular interaction is taken into account. τ^{ex} represents the experimental values of the EET time. EET times τ^{GM} and τ^{PM} were obtained by solving GME and PME, respectively.

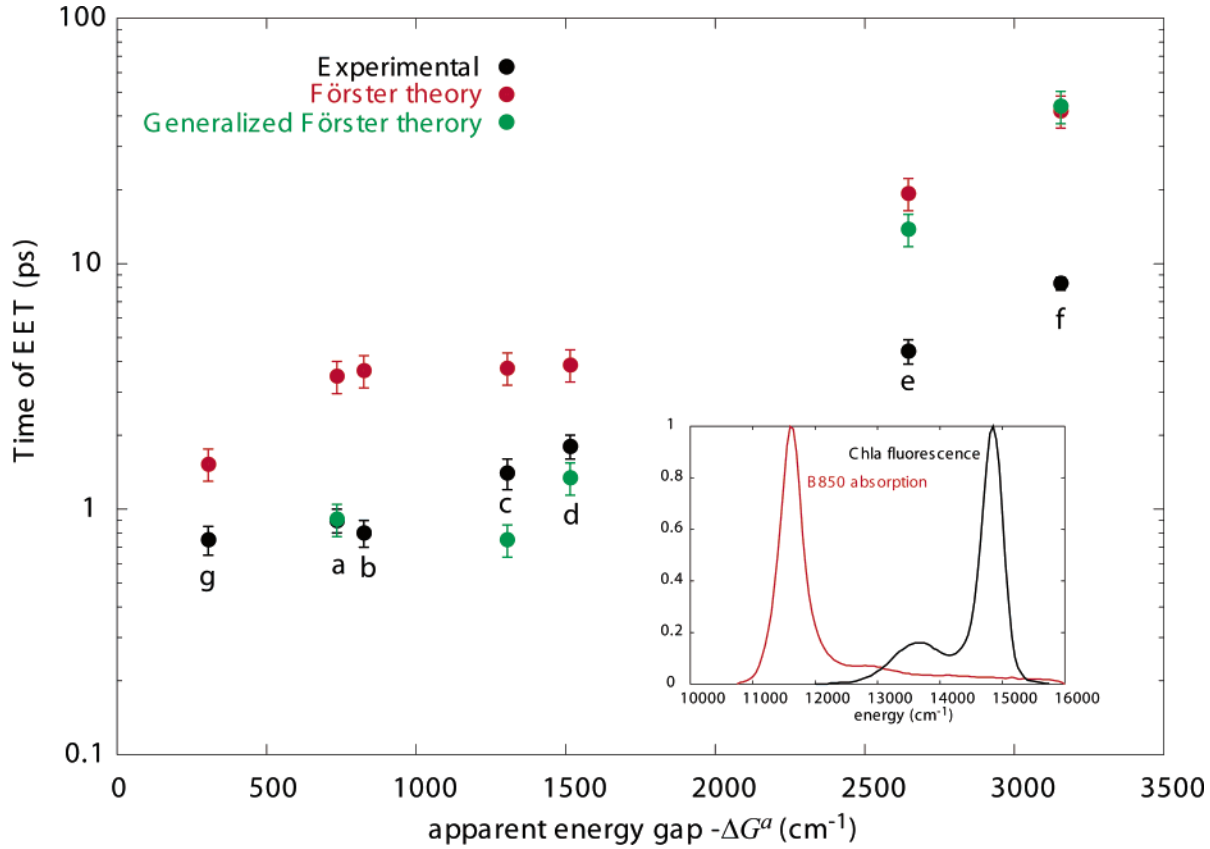

Figure 1. Apparent energy gap dependence of EET time for reconstituted B800 → B850 in LH2 (a−f) and LH3 (g) of *Rps. acidophilla*. The experimental values are plotted by black circles with error bars. The calculated values using the simple Förster theory (eq 1) are plotted by red circles with error bars. The values calculated by the generalized Förster theory and by considering the inhomogeneous effect of the spectra[14] are plotted by green circles with error bars.

nm. These results, together with the observed EET time, are summarized in Table 1.

Now, we define the apparent energy gap $-\Delta G^a$ as the difference between the fluorescence energy at the B800 site (donor site) and the absorption energy of the allowed exciton state of the B850 site (acceptor site). The fluorescence maximum wavelengths are calculated as the 80-cm^{-1} red shift from the absorption maximum wavelengths.[20] Those values are also listed in Table 1.

The logarithm of the experimentally obtained EET time is plotted by black circles as a function of the apparent energy gap for these six kinds of reconstituted LH2 in Figure 1a−f. We see that the EET time increases almost exponentially with the apparent energy gap except for the small energy gap.

Herek et al. tried to reproduce these data by the calculation using the Förster theory in a simplified manner.[18] Namely, they treated the interaction between B800 and B850 as a dipole−dipole interaction by assuming that the coherent exciton state

of the B850 ring has a transition dipole moment as a whole. Then, they used the equation

$$k_{i\rightarrow j} = \frac{4\pi^2}{h^2 c} U^2 \int \left[\frac{F_i(\nu)}{\nu^3}\right]\left[\frac{A_j(\nu)}{\nu}\right] d\nu = 1.18 U^2 \Theta \quad (1)$$

where $k_{i\rightarrow j}$ is the EET rate between donor (i) and acceptor (j) molecules (ps^{-1}), U is the transition dipole−transition dipole interaction between them (cm^{-1}), and Θ is the overlap integral between the donor fluorescence spectrum $F_i(\nu)$ divided by ν^3 and the acceptor absorption spectrum $A_j(\nu)$ divided by ν, for which the intensities (area) have been normalized to unity on the cm^{-1} scale.[21]

The calculated values (a−f) are plotted by red circles with error bars of 15%, allowing for signal−noise limitations in the emission spectra and uncertainties in estimating U values (∼30 cm^{-1} for native complexes) and the Stokes shift.[18] U^2 values in the complexes reconstituted with 3-vinyl-BChla, 3′-OH−BChla, 3-acetyl-Chla, and Chla were 0.88, 0.92, 0.74 and 0.52 times larger than those in LH2, respectively.[18] We find that the calculated data qualitatively reproduce the essential character of the energy gap dependence of the experimentally obtained EET time. We also find that the calculated values of the EET time for the donors expressed by symbols a, b, e, and f are systematically about 5 times larger than those of the experimental data.[18] The calculated values of the EET time for donors expressed by symbols c and d are 2.7 and 2.2 times larger, respectively, than those of the experimental data.[18] It should be noticed that the EET rate calculated using eq 1 is not as small as expected before[12] because the long tail of the absorption spectrum of B850 on the shorter-wavelength side contributes to the enhancement of the overlap integral with the fluorescence spectrum of the reconstituted B800. In this Figure, we added one more point, expressed by the symbol *g*, that is the EET time for B800 → B820 in LH3.[22] In this case, the maximum fluorescence wavelength of B800 is close to the maximum absorption wavelength of B820, and the calculated EET time becomes very small. However, the experimental data of the EET time do not differ among a, b, and g, and the calculated EET time for g is only 2 times larger than the experimental data. These results indicate that the calculated EETs using eq 1 by assuming the exciton state of B850 as an acceptor are within the range of 2−5 times the experimental values.

To eliminate the systematic displacement of the calculated values from the experimental data, the magnitude of the dipole−dipole interaction would have to be 2−2.5 times larger than the correctly estimated value (∼30 cm^{-1}).[18] It has been suggested previously that the carotenoid would contribute to the enhancement of the coupling between B800 and B850.[21,23,24] More recent calculations indicate that the enhancement by the carotenoids is at most 10−20 cm^{-1}, which is not sufficient to eliminate the discrepancy.[25] It has been also pointed out that the multipole−multipole interactions, which become effective when the size of the donor and acceptor molecules is comparable to the donor−acceptor distance, will facilitate the excitation energy transfer to an optically forbidden exciton level (generalized Förster mechanism).[13−15] If these couplings were the source of the disagreement between the calculated and measured rates, then we would expect the mismatch to be larger for those substituents whose absorption bands lie within and outside the exciton manifold of B850. Because the difference between the calculated and measured rates in all of the complexes is around a factor of 5, such coupling terms cannot be responsible for the discrepancy.[18] Indeed, the EET times corresponding to cases a, c, d, e, and f in Table 1 calculated by the generalized master equation are 0.76, 1.06, 2.17, 16.,9 and 62.3 ps, respectively, in the absence of disorder and 0.91, 0.75, 1.34, 13.8, and 43.7 ps, respectively, in the presence of disorder.[14] Those values calculated in the presence of disorder are plotted in Figure 1 by green circles with error bars. We find that the apparent energy gap dependence of the calculated EET times is much stronger than that of the experimental values. The calculated EET times for cases e and f corresponding to the larger energy gaps are much larger than the experimental values. Hence, we conclude that the generalized Förster theory fails to reproduce the experimental data of the energy gap dependence of the EET of reconstituted B800 → B850.

2. Theoretical Model

In this paper, we propose a new theoretical model to resolve the discrepancy described above between the theoretical calculations and the experimental data. We also propose a new mechanism for the EET of B800 → B850. To clarify the motivation for this analysis, we first present the most simplified model. Phenomenologically, let us consider the case in which the rate-limiting step for EET of B800 → B850 is EET from B800 to the BChla in B850 closest to the photoexcited BChla in B800. Considering that the value of U in B850 is around 300 cm^{-1},[8] we estimate the site energy of BChla in B850 to be about 810 nm, by which the optically allowed exciton band of B850 is reproduced at 850 nm. This site energy is considerably larger than that of the excitonic absorption maximum wavelength of B850. Therefore, the overlap between the absorption spectrum of monomeric BChla in B850 and the fluorescence spectrum of reconstituted B800 is increased considerably compared to the overlap in the above calculations using the exciton absorption spectrum of B850. Accordingly, the EET rate will be increased systematically, and the discrepancy between the calculated values and the experimental values will be decreased.

Before going into a detailed discussion of the origin of such a mechanism for EET of B800 → B850, let us evaluate the EET rate on the basis of a more refined theoretical base in line with the above idea.

We adopt the generalized master equation (GME) method as follows:[26]

$$\frac{dP_i(t)}{dt} = \sum_{j\neq i} \int_0^t dt_1 [M_{ij}(t, t_1) P_j(t_1) - M_{ji}(t, t_1) P_i(t_1)] \quad (2)$$

where $P_i(t)$ is the probability that pigment i is excited at time t. $M_{ij}(t, t_1)$ is the memory function representing the probability that pigment j is excited at time t_1 and that pigment i is excited at a later time t by excitation-energy transfer from pigment j to pigment i. This GME is exact if the memory function is chosen correctly. Indeed, we obtain a pure exciton state when $M_{ij}(t, t_1)$ is a constant (ca. $2U_{ij}^2/\hbar^2$). In the present study, we adopt second-order perturbation theory to evaluate $M_{ij}(t, t_1)$ as follows:[27]

$$M_{ij}(t, t_1) = \frac{2U_{ij}^2}{\hbar} \int_{-\infty}^{\infty} d\left(\frac{\Delta E}{\hbar}\right) \cos\left[\frac{\Delta E(t - t_1)}{\hbar}\right] \times \int dE' L_j\left(E, E', \frac{t + t_1}{2}\right) I_i(E' - \Delta E) \quad (3)$$

where U_{ij} is the interaction energy between pigments i and j, $L_j(E, E', t)$ is the normalized fluorescence spectrum of molecule

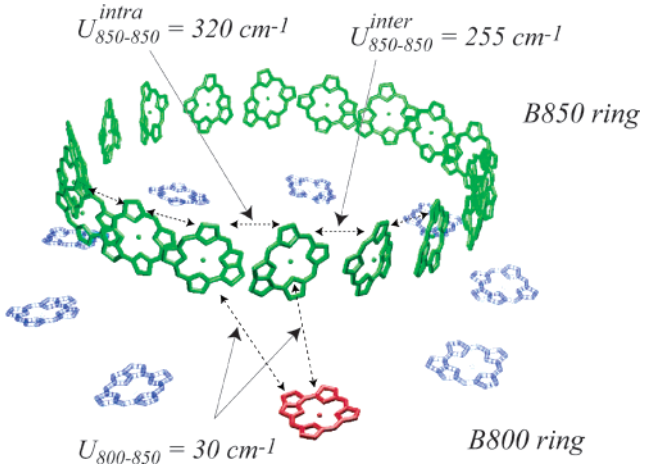

Figure 2. Configuration of the BChla molecules of the B850 and B800 rings. Two alternative kinds of intermolecular interactions, 320 and 255 cm^{-1}, are assumed to take place inside the B850 ring.[14] Two BChla molecules in the B850 ring are assumed to have an interaction, with an amplitude of 30 cm^{-1} (ref 14), with a nearby BChla molecule in the B800 ring.

j at time t, which is excited to energy level E at initial time $t = 0$, and $I_i(E')$ is the normalized absorption spectrum of molecule i. At the present time, we have little knowledge of the time dependence of the fluorescence spectrum. Therefore, we use the fluorescence spectrum obtained under the condition that the stationary state is attained in the excited state. The validity of this treatment in our system is discussed later. Then, we obtain

$$M_{ij}(t, t_1) = \frac{2U_{ij}^2}{\hbar} \int_{-\infty}^{\infty} \mathrm{d}\left(\frac{\Delta E}{\hbar}\right) \cos\left[\frac{\Delta E(t - t_1)}{\hbar}\right] \times \int \mathrm{d}E'\, L_j(E')\, I_i(E' - \Delta E) \quad (4)$$

Equation 4 is essentially the same as that obtained by Kenkre and Knox.[28] When $M_{ij}(t, t_1)$ is expressed by a δ function, the GME reduces to the Pauli master equation (PME), and EET takes place by the hopping mechanism or the Förster mechanism between the neighboring chromophores. Mathematically, this corresponds to the case in which only $\Delta E = 0$ is effective in the integrand of eq 4. In the GME of eq 4, we are not constrained to the case $\Delta E = 0$, so some coherent character is reserved in the transition. It should be pointed out that if we use the memory function of eq 4 and assume an independent inhomogeneous broadening effect on the absorption and fluorescence spectra then the absorption and fluorescence spectra involving the inhomogeneous broadening effect can be used in eq 4.[27] This assumption would be appropriate when donor and acceptor molecules are separated considerably. The BChla molecules in B850 are in rather close positions. In such case, the average for the inhomogeneous broadening effect should be taken for the product of the intrinsic absorption and fluorescence spectra, as was done by Scholes and Fleming.[14] Because we use the experimental data of absorption and fluorescence spectra in solution, we must adopt the above approximation.

In the following numerical calculations, we assume that the initial excitation energy is completely localized on one BChla molecule in B800. Two BChla molecules in the B850 ring are close to a BChla molecule in B800. Those interactions are estimated to be 30 cm^{-1} for both.[14] We assume two alternate kinds of interactions for the neighboring BChla's in B850 ring such as 320 and 255 cm^{-1}.[14] Those parameter values are drawn in Figure 2. The site energy of BChla in B850 is 12 340 cm^{-1} (810 nm). These values are used for all of the reconstructed LH2s.

The absorption spectrum shape $I_i(E)$ of a BChla in the absence of exciton coupling in B850 is taken from the absorption spectrum of BChla in solution.[29] In the literature, we do not find any fluorescence spectra of BChla accurate enough for the present analysis. Then, the shape of the fluorescence spectrum $L_j(E)$ of reconstituted B800 is substituted by that of Chla in solution except for the peak position.[18] The fluorescence spectrum of Chla and the absorption spectrum of BChla in reconstituted LH2 are shown in the inset of Figure 3. We find that both spectra exhibit long tails that enlarge the spectral overlap. The site energy gap $-\Delta G^s$, defined as the difference between the fluorescence energy of reconstituted B800 and the site energy of BChla in B850, is listed in Table 1. In this case, the relation $-\Delta G^s = -\Delta G^a - 581\ cm^{-1}$ holds.

3. Results

We calculate the time dependence of the decay of the population of reconstituted B800 by the GME and PME methods. We calculate the first passage time τ for EET using the GME and PME methods:

$$\tau = \frac{1}{P_{B800}(0) - P_{B800}(\infty)} \int_0^{\infty} (P_{B800}(t) - P_{B800}(\infty))\, \mathrm{d}t \quad (5)$$

The calculated EET times are listed in the right column of Table 1. We added a ±15% error width to account for ambiguity in the choice of spectral shapes and parameter values. We find that τ^{PM} is quite similar to τ^{GM}.

In Figure 3, we plotted the logarithm of τ^{GM}'s of the reconstituted LH2 together with the experimental data as a function of the apparent energy gap $-\Delta G^a$ using red and black circles with error bars, respectively. We find that the calculated values of the EET time fit the experimental values (a−f) very well over a wide range of the energy gap.

We also calculated the EET time for B800 → B820 in LH3. The site energy of BChla in B820 is estimated to be at 780 nm so that absorption maximum wavelength of the exciton band of B820 is reproduced using the same interaction parameters as B850. In this case, the EET is an virtually uphill transition. The parameter values and the calculated excitation energy transfer time by the GME and PME methods are listed in Table 2. The calculated EET time τ^{GM} is plotted in Figure 3 by symbol g. In this case, the agreement between the calculated value and the experimental value is also very good, and τ^{GM} agrees well with τ^{PM}.

In such a way, we could reproduce the experimental data of the energy gap dependence of the reconstituted B800 → B850 EET very well by the GME with a memory function in eq 4. Furthermore, we obtained almost the same values between τ^{PM} and τ^{GM}. These results indicate that the EET of B800 → B850 proceeds in a manner in which the excitation energy of BChla in B800 is first transferred to BChla molecules in B850, which are close to the excited BChla in B800. The totally delocalized exciton state of B850 is not used in this EET.

4. Discussion

Let us consider the reason that the EET of B800 → B850 is essentially described by the GME with use of the second-order memory function and almost by the PME, although the delocalized exciton band of B850 is observed in the optical absorption. In other words, why is the delocalized exciton band of B850 not used effectively in the EET of B800 → B850? In

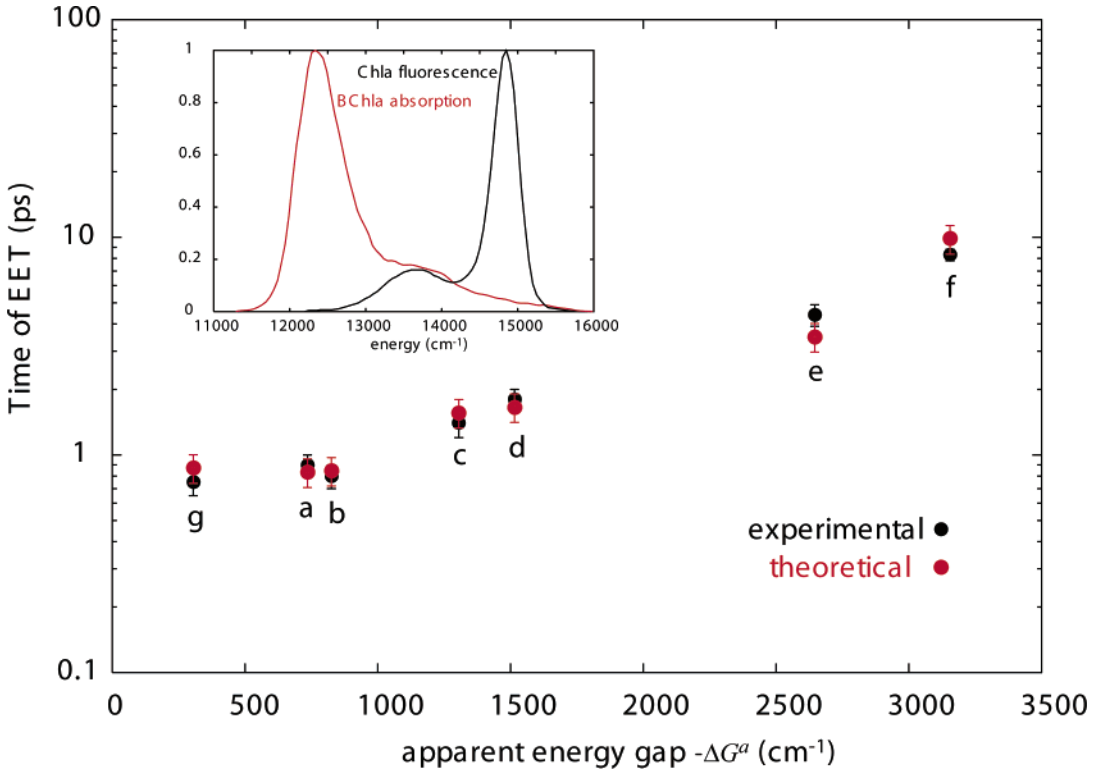

Figure 3. Apparent energy gap dependence of the experimental and theoretical values of EET times for reconstituted B800 → B850 as represented by black circles and red circles, respectively, with error bars. The theoretical values are calculated by GME using the memory function of eq 4. The inset shows the experimental data of the fluorescence spectrum of chlorophyll a[18] and the absorption spectrum of bacteriochlorophyll a in solution.[28] The Q_x band is deleted from the fluorescence spectrum.

TABLE 2: Summary of the Experimental Data of the Q_y Absorption and Fluorescence Maxima Wavelengths and the EET Time of LH3 in *Rps. Acidophilla* Taken from Referece 29[a]

B800 Site (Donor Site)

symbol	pigment	λ_{max}^{abs} (nm)	λ_{max}^{fl} (nm)	apparent energy gap $-\Delta G^a$ (cm^{-1})	site energy gap $-\Delta G^s$ (cm^{-1})	τ^{ex} (ps)	τ^{GM} (ps)	τ^{PM} (ps)
g	BChla	800	805	227	−399	0.75	0.87	0.88

B820 Site (Acceptor Site)

λ_{abs}^{max} (nm)	
exciton state	monomer state
820	780

[a] The others are the same as Table 1.

the following discussion, we shall show that the excitonic nature of the final state used in the optical absorption can be different from that used in the EET.

Qualitatively speaking, the coherent nature of the exciton state is promoted by excitonic coupling U between the chromophores because U works as a constructive force for excitonic coherence.[32] However, the coherent nature of the exciton state is decreased by the electron−phonon (vibration) interaction because the electron−phonon interaction works as a destructive force for excitonic coherence.[32] Whether the exciton state is stable is determined by the competition between these two kinds of forces.[32] When the constructive force prevails over the destructive force, the strong coupling regime applies, and the exciton domain length is expanded. When the two forces are comparable, the intermediate coupling regime applies, and the exciton domain length is decreased.[30,31] When the destructive force prevails over the constructive force, the weak coupling regime applies, and the excitonic character disappears. In the stationary state of the aggregate, the exciton domain length is determined by the balance of the total of both constructive and destructive forces.[32]

The manner of the constructive force that works to promote the coherent nature of the system also depends on the kind of observation. To see this clearly, let us consider the case of the optical absorption of the aggregate of chromophores. Before irradiation with incident light, all of the chromophores are in the ground state. After irradiation with incident light, a mixed state begins to be formed between the chromophore in the ground state plus a photon and the chromophore in the excited state.[31,34] While the mixed state is being maintained, the exciton state must be formed so that absorption by the exciton state might take place. The time for the mixed state to be maintained is determined by the nature of the destructive force, which we discuss in the next paragraph. The time for the formation of a dimer exciton is evaluated from the coherence communication time between the neighboring chromophores in the excited state. Using the uncertainty principle, the communication time T_c is around $\hbar/U$. Alternatively, we can estimate the communication

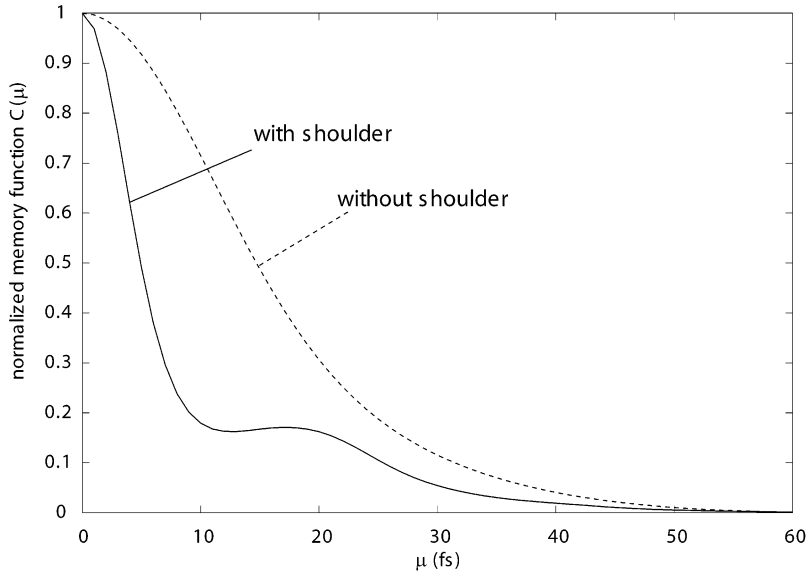

Figure 4. Time course of the normalized memory function $C(\mu)$ for the pair of BChla's with the same site energy in B850 (solid line). The optical absorption spectrum form of the BChla molecule and the fluorescence spectrum form of the Chla molecule in Figure 3 are used. The broken line is the time course of the normalized memory function obtained by subtracting the bump or shoulder in the absorption and fluorescence spectra.

time as a half period of the oscillation between neighboring chromophores, $h/4U$.[32] Such an evaluation of T_c using the dimer model might be considered to be a lower limit for the total communication time for the aggregate. This lower limit is true in the evaluation of the communication time for the aggregate in the stationary state. However, this evaluation of the total communication time for the aggregate is appropriate in the case of optical absorption. In the presence of incident light, the electronic states of all of the chromophores are simultaneously forced to oscillate in harmony with the incident-light frequency. This occurs because the incident light can induce the excitation of all of the chromophores with the same possibility so that the phase relation of an individual transition dipole moment to make the allowed transition dipole moment as the total becomes satisfied within almost the same time range as T_c. Therefore, an almost totally delocalized exciton state of the aggregate is formed by light absorption, as long as the condition for the dimer exciton being formed is satisfied. Putting $U = 300$ cm^{-1} on the average in B850, we obtain $\hbar/U = 16$ fs and $h/4U = 25$ fs. Therefore, we evaluate T_c in B850 as about 20 fs. Putting $U = 30$ cm^{-1} in the EET of B800 → B850, we evaluate T_c as about 200 fs.

Next, we discuss the problem of how we should characterize the destructive force. We consider the second-order memory function $M_{ij}(t - t_1)$ in eq 4 to be a possible physical quantity for this purpose. The amplitude of the memory function contributes to the motive force for the transition of population, and its time-dependence contributes to the memory of the population dynamics in the past. Then, we normalize $M_{ij}(t - t_1)$ as follows:

$$C_{ij}(\mu) = \frac{M_{ij}(\mu)}{M_{ij}(0)} \tag{6}$$

where $\mu = t - t_1$. We call $C_{ij}(\mu)$ a normalized memory function. $C_{ij}(\mu)$ contains only the properties of the optical absorption spectrum of the acceptor and the fluorescence spectrum of the donor. The normalized memory function $C_{ij}(\mu)$ represents the probability that the coherence is maintained after the passage of time μ. We can also say the following: $C_{ij}(\mu)$ has such a property that the excitonic coherence is destroyed rapidly when $C_{ij}(\mu)$ decays rapidly with μ and vice versa. This decay time T_D of $C_{ij}(\mu)$ represents the time that the chromophore maintains coherence. Therefore, the role of the destructive force can be measured by the inverse of the decay time T_D. In the following discussion, we drop the index ij from $C_{ij}(\mu)$ for simplicity.

We calculated $C(\mu)$ for the neighboring BChla's with a site energy of 810 nm in B850 using the absorption and fluorescence spectral forms in Figure 3. The result is drawn by the solid curve in Figure 4. We see that $C(\mu)$ initially decays very rapidly with a time constant T_D of about 6 fs, and then another broad peak follows, which decays with a time constant T_D of about 27 fs. A similar form of the normalized memory function was obtained even when the site energies of the two BChla's differed by about 2000 cm^{-1} in the fluorescence spectrum of Chla and the absorption spectrum of BChla, as seen in the inset of Figure 3.

The origin of the form of the normalized memory function in Figure 4 is as follows: The absorption spectrum has a large shoulder or bump in the energy region centered about 1200 cm^{-1} higher than that of the main peak. This shoulder or bump is due to the creation of one quantum of high-frequency vibrational modes during the optical transition. These modes would be made of mostly stretching motions of the π-conjugated skeletons in those molecules. To elucidate the origin of the broad side peak in $C(\mu)$, we subtracted the shoulder from the absorption spectrum of BChla and subtracted the bump from the fluorescence spectrum of Chla. The calculated $C(\mu)$ using the truncated spectra is plotted by the broken line in Figure 4. We see that only the slowly decreasing curve with a time constant of about 20 fs remains. Comparing the original $C(\mu)$ (solid curve) with this $C(\mu)$ (broken curve), we can say that the original $C(\mu)$ is much more concave in the early time region because of the presence of the large shoulder and the large bump in the absorption and fluorescence spectra. After about 20 fs, the decrease in $C(\mu)$ is diminished considerably, and the height of mostly about half of the broken curve is retained.

Now, let us discuss the problem of why the totally delocalized exciton state was observed in the optical absorption of B850. Comparing the two time constants (6, 27 fs) of T_D described above with T_c (~20 fs), we find that T_D for the initial fast decay of $C(\mu)$ is smaller than T_c, indicating that the memory time for

the formation of the dimer exciton is too short. We also find that T_D for the decay of the second peak is larger than T_c, indicating that the memory time for the formation of the dimer exciton is long enough. In the optical absorption, the condition for the formation of the dimer exciton is sufficient for the formation of the totally delocalized exciton state. Then, the second peak in the memory function can contribute to the formation of the almost totally delocalized exciton state of B850. Combining the contributions of the first and second peaks in the memory function, we can say that the mechanism of the optical absorption by B850 is a mixture of monomer excitation and delocalized exciton excitation. If the delocalized exciton state is formed in B850, then its absorption spectrum will be sharpened by the motional narrowing effect, and the second peak of the memory function will become larger than that in Figure 4. Then, the delocalized exciton excitation will become predominant in the optical absorption. In such a way, we can predict the observation of the 850-nm exciton band as the main peak. The long tail in the short-wavelength side of the main peak as observed in the experiment will represent a trace of the possible contribution from monomer excitation.

Now, let us move on to the mechanism of EET in B800 → B850. We have demonstrated that the experimental data of this EET can be well explained by the following theoretical scheme. The incident light is first absorbed by a BChla molecule in B800. This excitation energy is delivered to the nearby BChla molecules in B850, and then it is successively delivered to the other BChla molecules in B850. Its reasoning is considered as follows. In the mixed state of the initial and final states for the transition of B800 → B850, there is no chance for all of the BChla molecules in B850 to be excited at the same time, so the formation of the proper phase relation among the transition dipole moments of individual BChla molecules in forming the delocalized exciton state takes a long time. Here we assume that when the communication time for the dimer is T_c (20 fs) the communication time for the trimer will be about $2T_c$ (40 fs) and so on.[32] In the present case, the initial decay time T_D (6 fs) of $C(\mu)$ in Figure 4 is smaller than T_c. Therefore, this part contributes to the monomer excitation due to EET. The decay time T_D (27 fs) of the second peak in $C(\mu)$ is longer than T_c and is shorter than $2T_c$. This fact indicates that the memory time is long enough to form the dimer exciton but is too short to form the trimer exciton. On the basis of these results, we can say that EET from B800 to B850 will take place by means of the mixed mechanism of monomer excitation and dimer exciton excitation in B850. Because the height of the second peak of $C(\mu)$ in Figure 4 is considerably smaller than that of the first peak, we deduce that monomer excitation will make a more important contribution to EET than dimer excition excitation. Namely, the stepwise excitation energy transfer between BChla molecules virtually applies to B800 → B850.

In obtaining the second-order memory function of eq 4, we used the fluorescence spectrum emitted from the vibrationally relaxed excited state. Strictly speaking, this treatment would not be appropriate for the excited state of BChla molecules in B850 because the excitation energy transfer between the BChla molecules in B850 would be much faster than the vibrational relaxation rate. In such case, hot luminescence spectrum $L_j(E, E', (t + t_1)/2)$ in eq 3 should be used. The peak of the hot luminescence spectrum is located at a larger energy than that of the stationary fluorescence spectrum. However, its shift is at most 80 cm^{-1} as evaluated from the Stokes shift of 80 cm^{-1}.[20] The effect of this amount of spectral shift on the normalized memory function is small. The other property of the hot luminescence spectrum is that the width of the spectrum changes with time. Initially, the vibrational wave packet is produced around the Franck−Condon state. This vibrational wave packet propagates on the potential energy surface in the excited state. The vibrational wave packet become broadened on the way. In going to the end of vibrational relaxation in the excited state, the vibrational wave packet shrinks again to almost the original width of the wave packet. The fluorescence spectrum from such a vibrational state would broaden at first and shrink in the end. The effect of such a change in the fluorescence spectrum would shift the position of the second peak in Figure 4 to the smaller time, decreasing the value of T_c for the second peak. However, its effect is considered to be small because the vibrational relaxation energy is small in this system.

In the above discussion, we used the second-order memory function. Recently, we developed the EET theory by the GME method by introducing the renormalization of the memory function.[27] This renormalization includes all of the effects of higher-order perturbations of excitonic coupling U within the dimer. We showed that the renormalization effect is substantial for the memory function when we used the Lorentzian form of absorption and fluorescence spectra.[27] We calculated $C(\mu)$ by adopting such a renormalization effect in the present system. Surprisingly, the calculated $C(\mu)$ using the renormalization effect fits $C(\mu)$ calculated without the renormalization effect very well. The reason that the renormalization effect plays a much smaller role in our system is due to the specific spectra with bumps or shoulders attributable to BChla and Chla.

After the optical absorption of light by the delocalized exciton state of B850, the coherent domain length will shorten because no external force exists to promote the appropriate phase relation among the transition dipole moments of individual BChla molecules. It is theoretically predicted that a new stationary state with the time constant of 100−200 fs[34,35] is attained by the use of Redfield theory.[36] The exciton domain length N_{coh} in the stationary state was then predicted to be about 4.[34,35] The experimental data by the superradiance measurement suggested that $N_{coh} \approx 2.8$ at room temperature.[36] Our theoretical calculation in the present study indicates that $N_{coh} \approx 2$, so our value is a little smaller than the experimental value. The reason that our value is a little smaller than the experimental value might be due to our theoretical calculation using the GME theory in which the localized excited states are taken as a base and the excitonic coupling U is treated by the perturbation method. Therefore, our theoretical calculation is likely to underestimate the excitonic domain length. The fact that the experimental value of the excitonic domain length of B850 is much smaller than 18 units and is rather close to our result supports the validity of our treatment in this system. We can say that one is likely to overestimate the exciton domain length in the steady state in the theoretical analysis based on the Redfield theory in which the delocalized exciton state is taken as a base and the electron−phonon interaction is treated by the perturbation method.

The above discussion is summarized as follows: The absorption spectrum of BChla has a broad shoulder on the shorter-wavelength side. The fluorescence spectra of Chla have a large bump that is ∼1200 cm^{-1} lower in energy than the main peak. As a result of these specific spectra, the memory function decays very rapidly with time as compared with the memory function obtained using the optical spectra without a bump or shoulder. The excitation energy transfer from the locally excited state of B800 to B850 takes place mostly by means of the monomer excitation in B850. Even for such a situation, the optical absorption of B850 takes place mostly by means of the totally

delocalized exciton excitation because simultaneous coherent communication among all of the BChla molecules in B850 to form the delocalized exciton is possible in the course of the optical absorption. Then, we can say that the adoption of the exciton state as a base is suitable for the optical absorption and nonlinear optics, as carried out in most of the studies.[34,35] However, the adoption of the localized excited state of the chromophore as a base is suitable for EET of B800 → B850, as we have done in this study by means of the GME method. We can generalize the above result as follows: When the optical absorption or fluorescence spectra has a large bump or broad shoulder, the memory function decays very rapidly. In such case, the highly delocalized exciton state does not form easily in the stationary state. In such situation, EET can be described more properly by the GME or PME than by Redfield theory. This result supports the recent theoretical treatment of EET of PSI antenna systems by the PME.[37−39]

5. Conclusions

The experimental data of the energy gap dependence in the EET time of reconstituted B800 → B850 was well reproduced by calculations using GME theory with the memory function obtained by the second-order perturbation method. According to this result together with the analysis of the memory function, we may say that the rate-limiting step of this EET is a transition process from the localized state of B800 to the nearby BChla molecules with a site energy of 810 nm in B850. This result is related to the fact that the exciton domain length in the stationary state of B850 is as small as 2.8 BChla units, which was obtained by the superradiance experiment. A possible reasoning for this small exciton domain length is the very rapid decay of the memory function due to the existence of the large bump on the short-wavelength side of the main peak of the optical absorption spectrum of the BChla molecule, which effectively broadens the whole spectral shape. The reason that the totally delocalized exciton band was observed by optical absorption is that all of the BChla molecules have an equal chance of being excited during their residence in the mixed state in the absorption of light, and it is possible to form the totally delocalized exciton state even under the condition that only the dimer exciton is formed in the stationary state. It follows that the coherence domain length in the final state that one looks at via optical absorption is much larger than what one looks at by the measurement of EET. On the basis of the present results, we can say in general that the coherence domain length of the BChla (Chla) aggregates in the stationary excited state is very small and that the generalized master equation and possibly the Pauli master equation can be used to calculate the EETs of most of the photosynthetic antenna systems.

Acknowledgment. This work was supported by a Grant-in-Aid for Scientific Research (C) for T. K. from the the Ministry of Education, Culture, Sports, Science and Technology of Japan.

References and Notes

(1) van Amerongen, H.; Valkunas, L.; van Grondelle, R. *Photosynthetic Excitons*; World Scientific: Singapore, 2000.

(2) Renger, T.; May, V.; Kühn, O. *Phys. Rep.* **2001**, *343*, 137.

(3) McDermott, G.; Prince, S. M.; Freer, A. A.; Hawthornethwaite-Lawless, A. M.; Papiz, M. Z.; Cogdell, R. J.; Isaccs, N. W. *Nature* **1995**, *374*, 517.

(4) Sundström, V.; Van Grondelle, R. In *Anoxygenic Photosynthetic Bacteria*; Blankenship, R., Madigan, M. T., Bauer, C. E., Eds.; Kluwer: Dordrecht, The Netherlands, 1995; pp 349−372.

(5) Sauer, K.; Cogdell, R. J.; Prince, S. M.; Freer, A.; Isaacs, N. W.; Scheer, H. *Photochem. Photobiol.* **1996**, *64*, 564.

(6) Pullerits, T.; Sundström, V. *Acc. Chem. Res.* **1996**, *29*, 381.

(7) Hu, X.; Ritz, T.; Damjanović, A.; Schulten, K. *J. Phys. Chem. B* **1997**, *101*, 3854.

(8) Sundström, V.; Pullerits, T.; van Grondelle, R. *J. Phys. Chem. B* **1999**, *103*, 2327.

(9) van Oijen, A. M.; Ketelaars, M.; Köhler, J.; Aartsma, T. J.; Schmidt, J. *Science* **1999**, *285*, 400.

(10) Ketelaars, M.; van Oijen, A. M.; Matsushita, M.; Köhler, J.; Schmidt, J.; Aartsma, T. J. *Biophys. J.* **2001**, *80*, 1591.

(11) Matsushita, M.; Ketelaars, M.; van Oijen, A. M.; Köhler, J.; Aartsma, T. J.; Schmidt, J. *Biophys. J.* **2001**, *80*, 1604.

(12) Jimenez, R.; Nakshit, S. N.; Bradforth, S. E.; Fleming, G. R. *J. Phys. Chem.* **1996**, *100*, 6825.

(13) Mukai, K.; Abe, S.; Sumi, H. *J. Phys. Chem. B* **1999**, *103*, 6096.

(14) Scholes, G. D.; Fleming, G. R. *J. Phys. Chem. B* **2000**, *104*, 1854.

(15) Sumi, H. *J. Phys. Chem. B* **1999**, *103*, 252.

(16) Nagae, H.; Kakitani, T.; Katoh, T.; Mimuro, M. *J. Chem. Phys.* **1993**, *98*, 8012.

(17) Shreve, A. P.; Trautman, J. K.; Frank, H. A.; Owens, T. G.; Albrecht, A. C. *Biochim. Biophys. Acta* **1991**, *170*, 231.

(18) Herek, J. L.; Fraser, N. J.; Pullerits, T.; Martinsson, P.; Polivka, T.; Scheer, H.; Cogdell, R. J.; Sundström, V. *Biophys. J.* **2000**, *78*, 2590.

(19) Leupold, D.; Stiel, H.; Ehlert, J.; Nowak, F.; Teuchner, K.; Voight, B.; Bandila, M.; Ücker, B.; Scheer, H. *Chem. Phys. Lett.* **1999**, *301*, 537.

(20) van Grondelle, R.; Kramer, H. J. M.; Rijgersberg, C. P. *Biochim. Biophys. Acta* **1982**, *682*, 208.

(21) Pullerits, T.; Hers, S.; Herek, J. L.; Sundström, V. *J. Phys. Chem. B* **1997**, *101*, 10560.

(22) Ma, Y.; Cogdell, R. J.; Gillbro, T. *J. Phys. Chem. B* **1998**, *102*, 881.

(23) Scholes, G. D.; Harcount, R. D.; Fleming, G. R. *J. Phys. Chem. B* **1997**, *101*, 7302.

(24) Krueger, B. P.; Scholes, G. D.; Fleming, G. R. *J. Phys. Chem. B* **1998**, *102*, 5378.

(25) Krueger, B. P.; Scholes, G. D.; Gould, I. R.; Fleming, G. R. *Phys. Chem. Commun.* **1999**, 8.

(26) Zwanzig, W. In *Lectures in Theoretical Physics*; Downs, W. E., Downs, J., Eds.; Interscience: Boulder, CO, 1961; Vol. 3.

(27) Kimura, A.; Kakitani, T. *J. Phys. Chem. B*, submitted for publication.

(28) Kenkre, V. M.; Knox, R. S. *Phys. Rev.* **1974**, *9*, 5279.

(29) Eichwurzel, I.; Stiel, H.; Teuchner, K.; Leupold, D.; Scheer, H.; Scherz, A. *Photochem. Photobiol.* **2000**, *72*, 204.

(30) Kimura, A.; Kakitani, T.; Yamato, T. *J. Phys. Chem. B* **2000**, *104*, 9276.

(31) Kakitani, T.; Kimura, A.; Sumi, H. *J. Phys. Chem. B* **1999**, *103*, 3720.

(32) Kakitani, T.; Kimura, A. *J. Phys. Chem. A* **2002**, *106*, 2173.

(33) Redfield, A. G. *Adv. Magn. Reson.* **1965**, *1*, 1.

(34) Kühn, O.; Sundström, V. *J. Chem. Phys.* **1997**, *107*, 4154.

(35) Dahlbom, M.; Pullerits, T.; Mukamel, S.; Sundström, V. *J. Phys. Chem. B* **2001**, *105*, 5515.

(36) Monshouwer, R.; Abrahamsson, M.; van Mourik, F.; van Grondelle, R. *J. Phys. Chem. B* **1997**, *101*, 7241.

(37) Damjanovic, A. A.; Vaswani, H. M.; Fromme, P.; Fleming, G. R. *J. Phys. Chem. B* **2002**, *106*, 10251.

(38) Sener, M. K.; Lu, D.; Ritz, T.; Park, S.; Fromme, P.; Schulten, K. *J. Phys. Chem. B* **2002**, *106*, 7948.

(39) Byrdin, M.; Jordan, P.; Krauss, N.; Fromme, P.; Stehlik, D.; Schlodder, E. *Biophys. J.* **2002**, *83*, 433.